



MODELICA

Proceedings
of the 4th International Modelica Conference,
Hamburg, March 7-8, 2005,
Gerhard Schmitz (editor)

E. Surewaard, M. Thele

Ford Forschungszentrum Aachen, RWTH Aachen University, Germany

Modelica in Automotive Simulations - Powernet Voltage Control during Engine Idle

pp. 309-318, updated, not published

Paper presented at the 4th International Modelica Conference, March 7-8, 2005,
Hamburg University of Technology, Hamburg-Harburg, Germany,
organized by The Modelica Association and the Department of Thermodynamics, Hamburg University
of Technology

All papers of this conference can be downloaded from
<http://www.Modelica.org/events/Conference2005/>

Program Committee

- Prof. Gerhard Schmitz, Hamburg University of Technology, Germany (Program chair).
- Prof. Bernhard Bachmann, University of Applied Sciences Bielefeld, Germany.
- Dr. Francesco Casella, Politecnico di Milano, Italy.
- Dr. Hilding Elmqvist, Dynasim AB, Sweden.
- Prof. Peter Fritzson, University of Linkping, Sweden
- Prof. Martin Otter, DLR, Germany
- Dr. Michael Tiller, Ford Motor Company, USA
- Dr. Hubertus Tummescheit, Scynamics HB, Sweden

Local Organization: Gerhard Schmitz, Katrin Prölb, Wilson Casas, Henning Knigge, Jens Vasel, Stefan Wischhusen, TuTech Innovation GmbH

Modelica in Automotive Simulations - Powernet Voltage Control during Engine Idle

Erik Surewaard
Ford Forschungszentrum Aachen
Suesterfeldstrasse 200
52072 Aachen, Germany
esurewal@ford.com

Marc Thele
RWTH Aachen University
Jaegerstrasse 17-19
52066 Aachen, Germany
marc.thele@isea.rwth-aachen.de

Abstract

Due to the increasing electric power demand of future vehicles, problems may be expected with the voltage stability of the powernet. In conventional vehicles, control of the powernet voltage can be lost when the loads in the electric powernet request more power than can be supplied by the generator. In that case voltage control of the powernet will be lost since the generator will not be able to follow the voltage setpoint. The voltage of the electric powernet will drop to and follow the battery voltage. This will go impaired with undesired voltage fluctuations resulting in light flicker and blower motor fluctuations, which can be noticed by the vehicle occupants. This will have a negative effect on customer perception.

This paper describes both physical plant models and control algorithms, which can be used for simulation of the electric powernet. By making use of the ModelicaVMA structure that has been set-up by Tiller *et. al.* in [1], a simulation model is set-up including detailed models of: (i) a battery, (ii) generator, (iii) heated front windscreen and (iv) an internal combustion engine. In the case of de-icing the front windscreen during engine idle, simulations have been performed to investigate what the effect is of (i) engine idle speed control and (ii) load switching compared with the conventional situation.

1 Introduction

The average electric power drawn in a conventional vehicle, shows a rising trend over the years. This is on the one hand caused by the growing amount of electric comfort loads but also by the electrification

of vehicle chassis functions, *e.g.* Electric Power Assisted Steering (EPAS) and Electronic Damping Control (EDC). Since the electric powernet will get an increasingly important function in the vehicle, electric load models will also become increasingly important for future vehicle simulations. That the Modelica language can be of great benefit in electric powernet simulations has already been shown by the author in [2], [3] and [4]. That Modelica is also suitable for control system development will be shown in an application for powernet voltage control during engine idle. Based on the ModelicaVMA structure, this paper describes physical models and control algorithms, which can be used to investigate voltage stability of the electric powernet during engine idle.

2 Powernet Voltage Stability

Fig. 1 shows a schematic of the powernet of a conventional vehicle in which the generator voltage is the only variable that can be actively controlled.

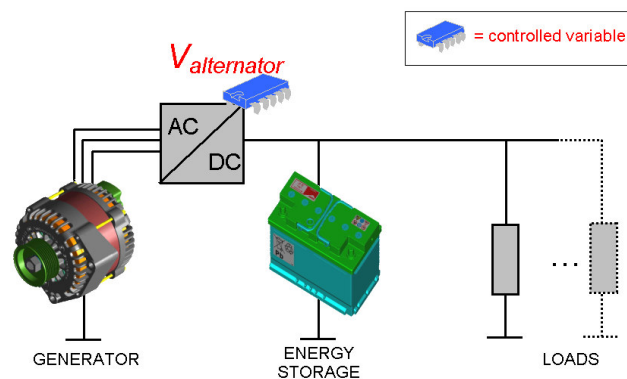


Fig. 1 Powernet topology for a conventional vehicle in which only the generator voltage can be controlled

Dependent on the amount of requested electric power by the loads, two powernet states can occur:

1. The powernet state in which the requested electric power is LOWER than the maximum that can be supplied by the generator. In this state the powernet voltage will be close to the voltage setpoint of the generator: in a conventional vehicle the voltage setpoint (*e.g.* 13.7V) of the generator is above the open circuit voltage of the battery (12.7V). Therefore the battery will be charged continuously in this state.
2. The powernet state in which the requested electric power is HIGHER than the maximum that can be supplied by the generator. In this state the additional requested power will be drawn from the battery. The saturated generator will not be able to follow the given setpoint and control of the powernet voltage will be lost: the powernet voltage will be determined by the battery. This will go hand in hand with voltage fluctuations which can be noticeable to the vehicle occupants: *e.g.* light flicker, changes in noise generated by the blower fan.

In conventional vehicles, the demand of electric power is usually highest during winter time when the engine is idling and the heated front screen is activated. The generator is usually saturated in this situation resulting in a loss of control of the powernet voltage. This paper will investigate means to prevent losing voltage control in this situation by using idle speed control or reducing the electric power to a load.

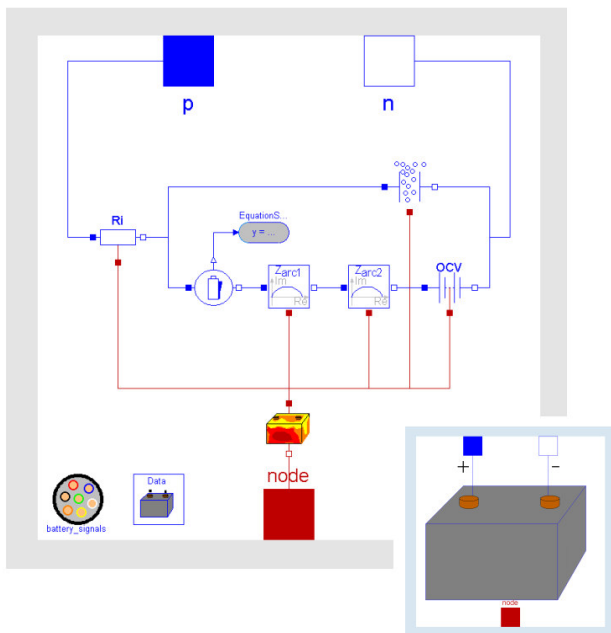
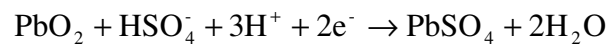


Fig. 2 Battery model as described in [3]

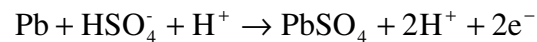
3 Battery

Fig. 2 shows the battery model that has been described by Surewaard in [3]. The issue with this model is that overcharging is not well described since the overcharging process is difficult to investigate with impedance measurements. The first step that is taken in the improvement of the battery model is to include the mass transport processes, which have been described by Thele in [5]. Mass transport processes will have a significant effect on the equilibrium voltage, also known as Open Circuit Voltage (OCV), of the battery. Detailed information on the Inclusion and research on the overcharging reaction is still in progress at the moment.

For a lead-acid (PbA) battery the discharge reaction that occurs at the positive electrode surface is the reaction of sulphuric acid and lead dioxide into lead sulphate and water whilst consuming two free electrons:



The discharge reaction that takes place at the negative electrode surface, is that lead and sulphuric acid react to lead sulphate and two hydrogen protons, forming two free electrons:



During charging above-mentioned reaction will take place in the opposite direction.

The reasons for including mass transport processes in the battery model are the following processes:

- **ACID FORMATION/CONSUMPTION AND DIFFUSION**
During discharging, sulphuric acid is consumed at the contact surface of both the positive and negative electrode. During charging sulphuric acid is formed at the electrode surfaces, which are in direct contact with the electrolyte. The differences in concentration will result in mass transport (diffusion) of sulphuric acid.
- **CHARGE MIGRATION**
This is the movement of charged particles (ions) due to the electric field that exists between the positive and negative electrode. HSO_4^- ions and electrons will be attracted by the positive electrode, H^+ protons will be attracted by the negative electrode.

3.1 Electrode Equilibrium Potential and Acid Formation/Consumption

The equilibrium potential of the positive and negative electrode is dependent on the acid concentration. According to Bode in [6], the molarity of sulphuric acid can be calculated from the sulphuric acid concentration by:

$$m = 1.00 \cdot 10^3 \cdot C + 3.55 \cdot 10^4 \cdot C^2 + 2.17 \cdot 10^6 \cdot C^3 + 2.06 \cdot 10^8 \cdot C^4 \quad (1)$$

in which C represents the acid concentration and m the molality. The electrode potential can now be calculated by the following equations:

$$u_+ = 1.628 + 0.0739 \cdot \log(m) + 0.0331 \cdot \log^2(m) + 0.0432 \cdot \log^3(m) + 0.0216 \cdot \log^4(m) \quad (2a)$$

$$u_- = -0.295 - 0.0736 \cdot \log(m) - 0.0305 \cdot \log^2(m) - 0.0305 \cdot \log^3(m) - 0.0120 \cdot \log^4(m) \quad (2b)$$

Acid formation/consumption at the electrode surface has been modeled with the following equations:

$$q_+ = \frac{3 - 2 \cdot t_+}{d \cdot A \cdot F \cdot 3600} \cdot i \quad (3a)$$

$$q_- = \frac{2 \cdot t_+ - 1}{d \cdot A \cdot F \cdot 3600} \cdot (-i) \quad (3b)$$

in which q_+ and q_- are the flows of acid ions, t_+ the transfer number for cations, d the electrode thickness, A the effective electrode surface, F the Faraday constant and i the current.

The above-mentioned equations have been implemented in a Modelica model for the positive and negative electrode of which Fig. 3 shows both top level icons.

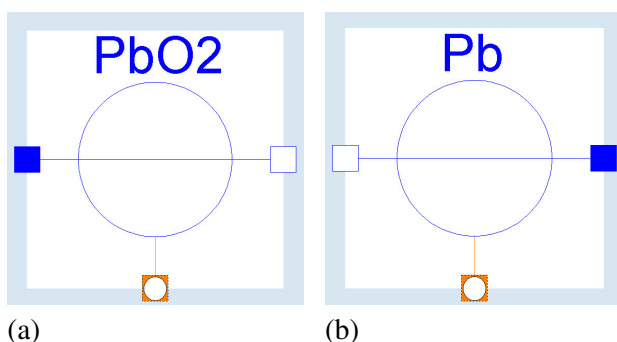


Fig. 3 Electrode equilibrium potentials which are dependent on acid concentration: (a) positive electrode, (b) negative electrode

In the figures the lower connector is the 'concentration' connector which has been defined as:

```
connector ConcentrationNode
  Modelica.SIunits.Concentration C
  "Concentration [mol/m3]";
  flow Real q(final unit="mol/s")
  "Diffusive flow";
end ConcentrationNode;
```

3.2 Electrode Porosity

Both the positive and the negative electrode have a porous structure, thereby increasing the surface area of the electrode with the bulk electrolyte. Due to the reaction that occurs during (dis)charging, the porosity of both electrodes will change. The maximum porosity of the electrode, *i.e.* the maximum amount of open space in the electrode, will be reached when the electrode is fully charged. Assuming the electrode porosity to be dependent on the battery State of Charge (SOC) and having a volume change as function of the amount of discharged energy, the electrode porosity has been described in a Modelica model. The top level icon of this model is displayed in Fig. 4a.

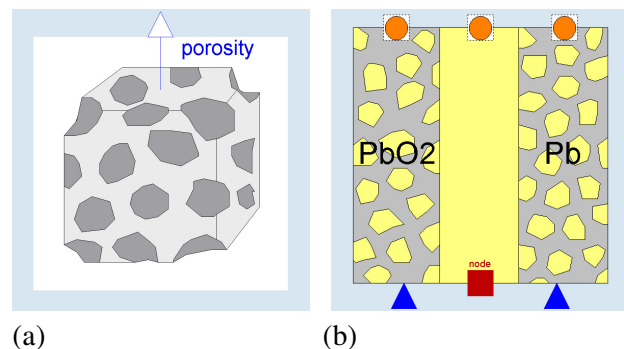


Fig. 4 Top level icon of the (a) electrode porosity model and (b) electrode-electrolyte diffusion model

3.3 Acid Diffusion and Charge Migration

For acid diffusion and charge migration, complex diffusion equations have been set-up based on equations described by Thele in [5]. These equations have been implemented in a Modelica model. The Modelica model, including all equations for acid diffusion and charge migration, is displayed in Fig. 4b. Three concentration connectors can be seen which from left to right represent (i) the positive electrode, (ii) the bulk electrolyte and (iii) the negative electrode. Since the diffusion processes are temperature dependent, the model contains a thermal connector. The inputs to the electrodes are their specific porosities, of which the model is discussed in the previous section.

3.4 Complete OCV Model

By combining the submodels that have been described in the previous subsections, the OCV model can be constructed, which is based on mass transport processes. This model is displayed in Fig. 5.

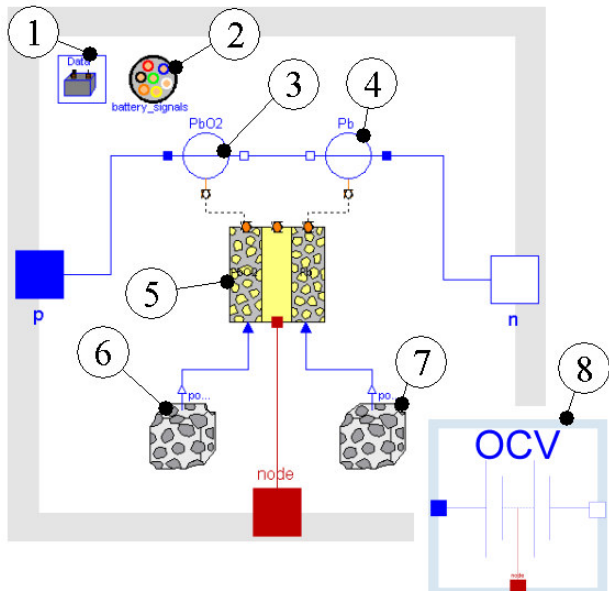


Fig. 5 OCV model including mass transport processes

The numbered submodels in Fig. 5 are a representation of: (1) battery parameters, (2) battery state information to be used for the porosity determination, (3) and (4) the equilibrium potential of respectively the positive and negative electrode, (5) the diffusion processes and charge migration, (6) and (7) the porosity of respectively the positive and negative electrode. Item (8) represents the top level icon.

The battery model that is described by Surewaard in [3] is extended with the OCV model based on mass transport processes by defining it as a replaceable. The parameter window for the battery model, including the replaceable OCV model, is displayed in Fig. 6. The already 'OCV_Simple' model is extended by the model described in this paper: 'OCV_MassTransportProcesses'.

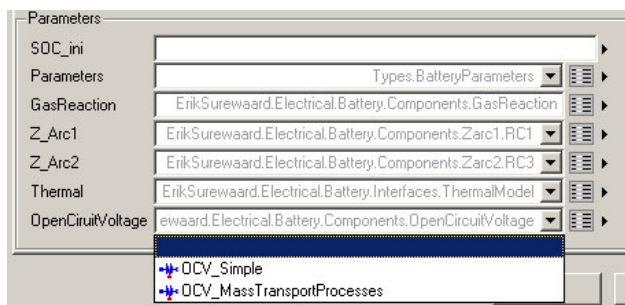


Fig. 6 Zoom of the parameter window of the battery model in which the OCV replaceable is highlighted

4 Heated Front Windscreen

A component in the electric powernet, which consumes a significant amount of electric power and has a relatively long thermal time constant, is the electrical heated front windscreen.

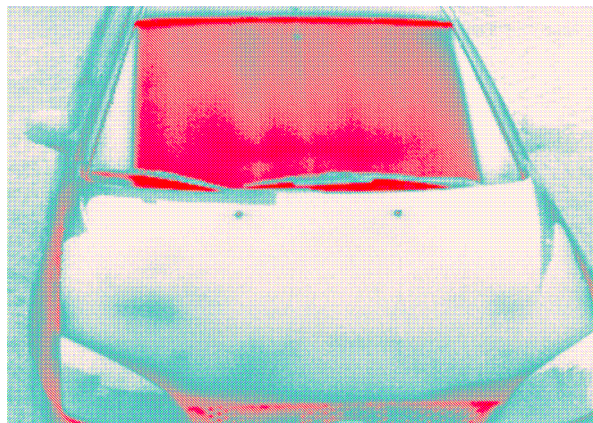


Fig. 7 Electric heated front windscreen: the area that is heated

The electric heated front windscreen basically consists of a sandwich of materials: a Polyvinyl Butyral (PVB) layer on which the tungsten heating wires are placed, sandwiched between two glass layers. A schematic of the layered structure is displayed in Fig. 8.

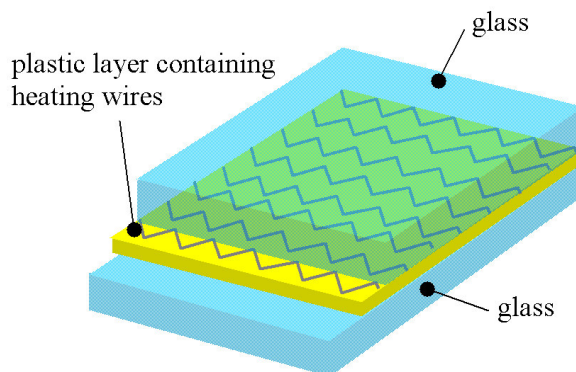


Fig. 8 Schematic overview of the different layers in an electric heated windscreen

The two-dimensional heat transfer model that is set-up for the electric heated windscreen is displayed in Fig. 9. Basically each material layer is modeled by taking the thermal mass in the center of the layer. The thermal mass is connected to the outer surface of the layer by it by two thermal conduction elements, each having half the thickness of the total layer.

Apart from components of the Modelica.Thermal.HeatTransfer library, two new components have been developed: (1) a thermal

mass representing the ice layer including the phase change from ice to water at 0°C , and (2) a thermal wire component, which converts electric power to a heat flow. The left and right thermal connectors in Fig. 9 represent respectively the inner and outer surroundings of the vehicle. Heat transfer between the screen surface and the surroundings takes place via both convection and thermal radiation.

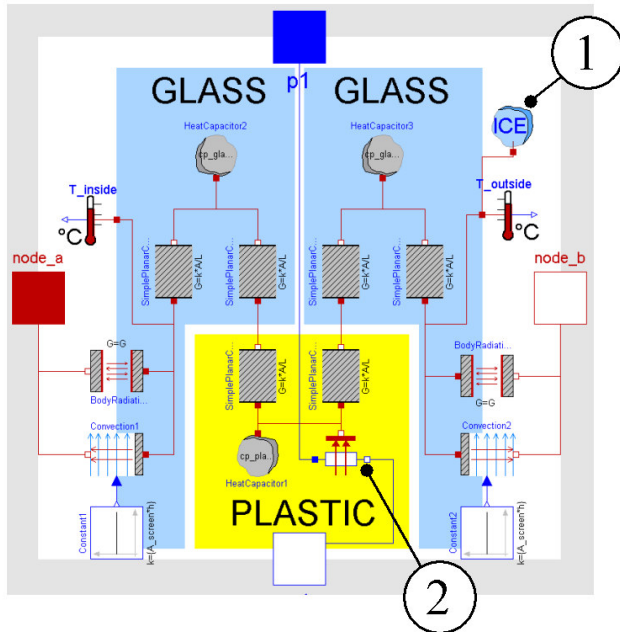


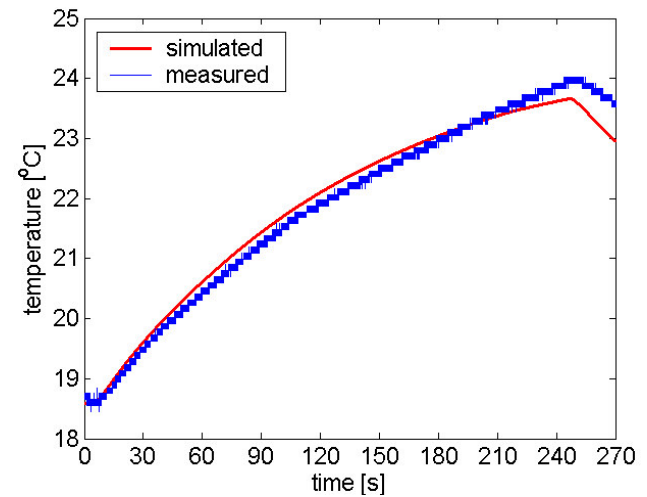
Fig. 9 Electro-thermal model for the electric heated windscreen

For the material constants and dimensions, use has been made of data supplied by the manufacturer of the heated screen and from literature. The model is validated by comparing simulated data with in-vehicle measured data with the electric heated windscreen active. The windscreen temperature is measured with a thermocouple attached to the inner surface of the windscreen (Fig. 10).

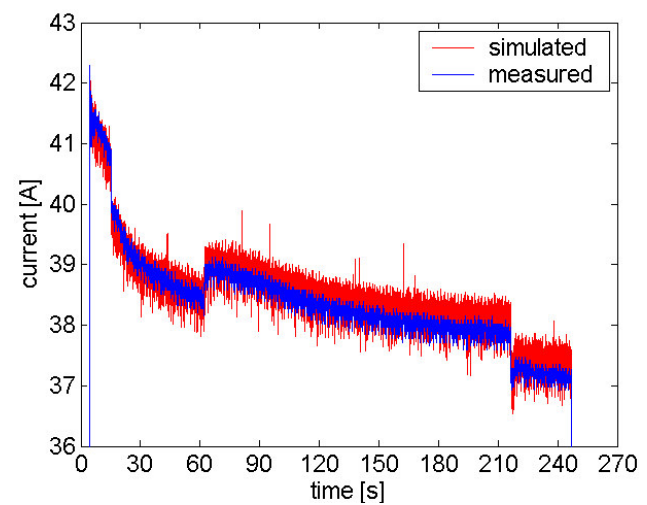


Fig. 10 Thermocouple attached to the inner surface of the windscreen

A measurement has been performed where the windscreen was initially at room temperature (approx. 18.5°C). The measured voltage at the terminals of the windscreen is used as input for the model. The simulated current and temperature have been compared with the measured current and temperature. The comparison of these results is displayed in Fig. 11 (heated windscreen was active in the timeframe between 5 and 250 seconds).



(a)



(b)

Fig. 11 Comparison between simulated and measured data of the heated windscreen: (a) temperature, (b) current

It can be seen from Fig. 11 that the simulated results correspond well with the measured data.

5 ModelicaVMA - Vehicle Idle Model

For the simulations, use will be made of the Vehicle Model Architecture (VMA), which is based on the description by Tiller in [1]. Since we are interested in

the engine idle state of the vehicle, the top level VMA model can be simplified to the one displayed in Fig. 12. The idle speed model contains the following physical plant and controller models: (1) driver, (2a) accessory drive, (2b) accessories controller, (3a) powerplant, (3b) powerplant controller, (4) transmission, (5a) electrical system, (5b) electrical system controller and (6) top level controller. The models of above-mentioned subsystems will be discussed in the following subsections.

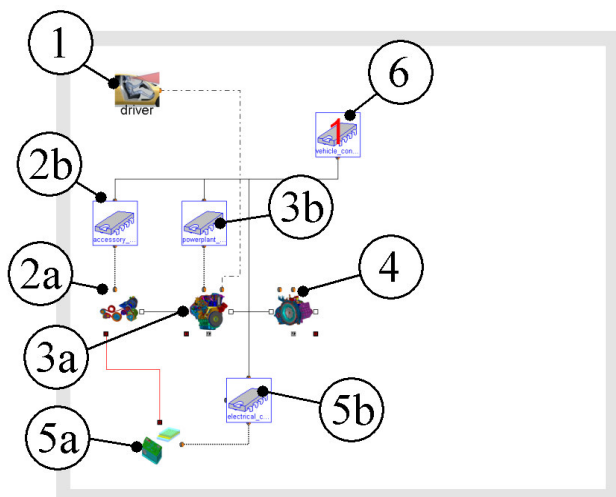


Fig. 12 Top level VMA model for the engine idle state

5.1 Driver

The driver subsystem is represented by item (1) in Fig. 12. Since the simulation will be performed with the engine idling, the driver subsystem will output a closed throttle position.

5.2 Accessories

The accessory subsystem and the accessory controller are represented by respectively items (2a) and (2b) in Fig. 12. The accessory subsystem includes a table lookup based generator model and also includes the belt losses. The top level icon of the accessory subsystem is displayed in Fig. 13a.

5.3 Powerplant

The powerplant subsystem and controller are represented by respectively items (3a) and (3b). An existing Simulink based model of an engine including its controllers (*e.g.* idle speed controller), which is used for fuel economy simulations at Ford, is converted to ModelicaVMA. The top level icon of the powerplant subsystem is displayed in Fig. 13b.

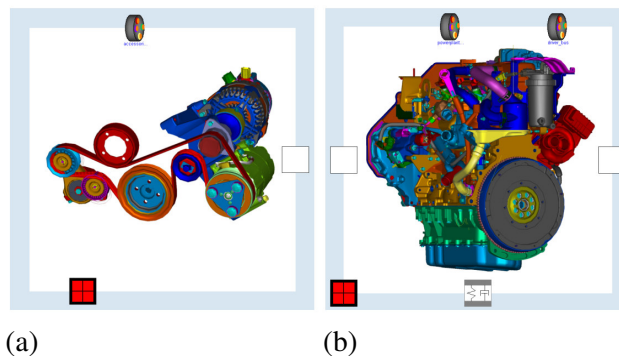


Fig. 13 Top level icons of (a) the accessory subsystem and (b) the powerplant subsystem

5.4 Electrical

The electrical subsystem and controller are represented by respectively items (4a) and (4b) in Fig. 12. The model of the electrical subsystem is displayed in more detail in Fig. 14 and includes the following models: (1) activation signal for the electrical windscreen, (2) switch of the electrical windscreen, (3) controllable PWM switch, (4) residual electrical loads, (5) battery, (6) heated windscreen and (7) top level icon of the electrical subsystem.

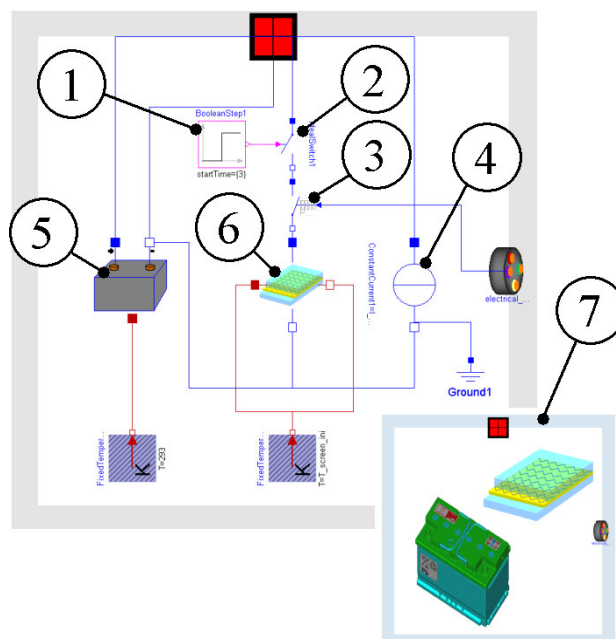


Fig. 14 Electrical subsystem containing battery, switches, heated windscreen and residual electrical loads

The strategy is to initiate the simulation with the heated windscreen inactive. After 3 seconds, the switch of the electrical windscreen will be closed so that it becomes active. The residual electrical loads are approximated by in-vehicle measured loads (having the electric heated screen inactive): 55A from 0-

100s, 40A during 100-200s and 20A after 200s. The reason for the high load current during the first 200 seconds is that the glow plugs are active (Diesel engine).

5.5 Transmission

The transmission subsystem is represented by item (4) in Fig. 12. For the idle speed simulations, it is modeled by having a closed clutch having the neutral gear engaged. The transmission subsystem includes both the engine and gearbox sided inertia and a table lookup model for the spinning losses in the neutral gear. The top level icon of the transmission subsystem is displayed in Fig. 15a.

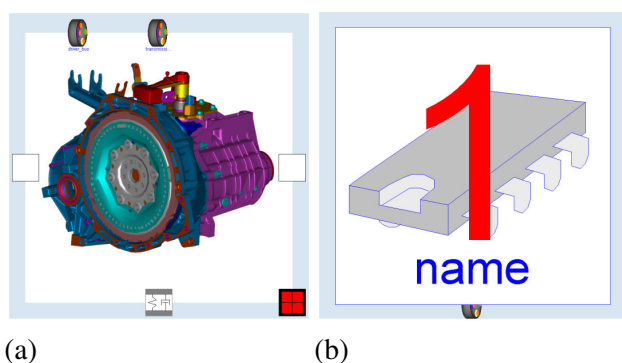


Fig. 15 Top level icons of (a) the transmission subsystem and (b) a top level controller implementation

5.6 Top level Controller

The top level controller is represented by item (6) in Fig. 12. Three top level controller models have been developed, each having a different voltage control strategy. The voltage control strategies will be discussed in the following section. The top level icon of one of the controllers is displayed in Fig. 15b.

6 Voltage Control Strategies

The top level controller, which is also known as the Vehicle System Controller (VSC), will control the idle speed of the engine, the voltage setpoint of the generator and if available the PWM frequency of the electric heated windscreen. Three control strategies will be investigated:

6.1 Strategy 1 - Conventional

Conventional 'strategy' where the idle speed is independent of the saturation of the generator. The engine idle speed setpoint will be 750 rpm.

NOTE: the PWM switch as displayed by item (3) in Fig. 14 is not used in this strategy.

6.2 Strategy 2 - Idle Speed Control

This strategy is based on the fact that the maximum generator output current can be increased if the idle speed is increased. The principle is displayed in Fig. 16. When the idle speed would be kept constant at say 750 rpm, the maximum output current will be approximately 70 A. When however the idle speed would be increased, the maximum generator output current also increases. Raising the idle speed above 1500 rpm would yield no benefits for the generator displayed in Fig. 16.

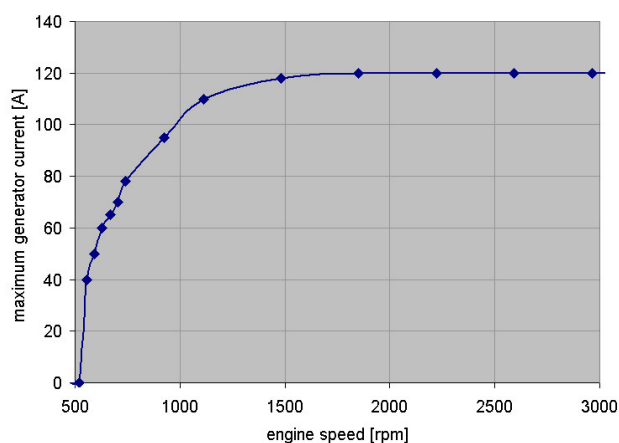


Fig. 16 Maximum generator output current as function of engine speed

The strategy that is implemented is that if the vehicle is in idle, the engine idle speed is controlled to reach a generator saturation of 95%. The window in which the idle speed is allowed to be changed is limited by a lower boundary of *e.g.* 750 rpm and an upper boundary of *e.g.* 1500 rpm (cf. Fig. 16).

NOTE: the PWM switch as displayed by item (3) in Fig. 14 is not used in this strategy.

6.3 Strategy 3 - Pulse Width Modulation

Pulse Width Modulation (PWM) switches can be added to specific electric loads in the powernet as has been proposed by for instance Graf in [7]. The powernet layout for this variant is displayed in Fig. 17.

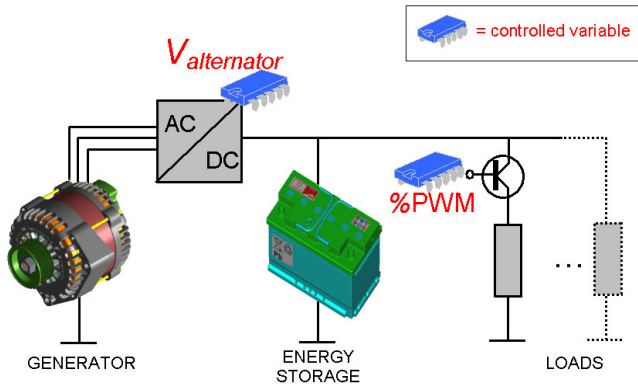


Fig. 17 Powernet variant in which next to the generator voltage also the electric power to a (group of) loads can be controlled

By adding a controllable PWM switch, an additional control variable is introduced in the electric power net next to the generator voltage. By reducing the electric power flowing to (a group of) loads, the total requested electric power can be controlled. In this way exceeding the maximum electric power that can be delivered by the generator can be prevented. According to Rienks [8], an approach is to add PWM switches to comfort loads, *e.g.* seat heating and screen heating, since these loads have a relative long time constant. Temporarily reducing the amount of electric power flowing to comfort loads will not affect customer acceptance as badly as losing control of the power net voltage and by that cause for instance light flickering.

In strategy 3, the PWM switch to the electric heated screen is controlled in such a way that the maximum output current of the generator is not exceeded: the power flowing to the heated screen is reduced to prevent the generator to saturate and loose control of the power net voltage. The engine idle speed setpoint is kept constant at 750 rpm in this strategy. The generator setpoint is set to 95%.

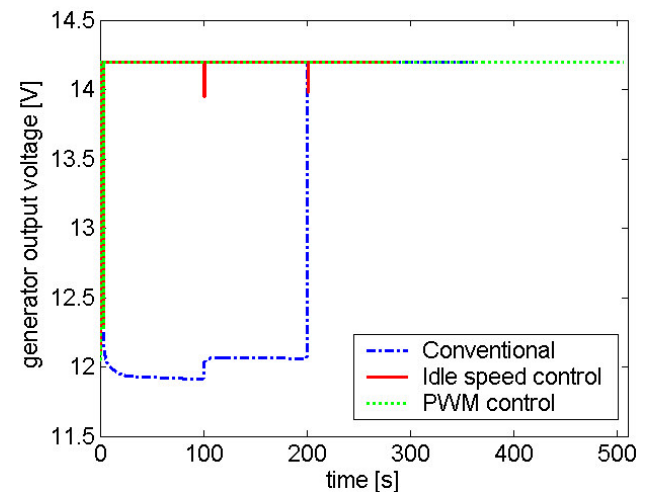
7 Simulation Results

One of the advantages of using the ModelicaVMA structure is the fact that all models can be redefined since they are defined as replaceable. The simulation results that will be described in this section, have been obtained by making use of the ModelicaVMA structure with the subsystem and controller models from Section 5 and the control strategies from Section 6. For the model parameters, use has been made of real vehicle data (Diesel engine, 120A generator and a 400W electrical heated front screen). A 12V lead-acid battery parameter set has further been used in the simulations: the initial battery State of Charge

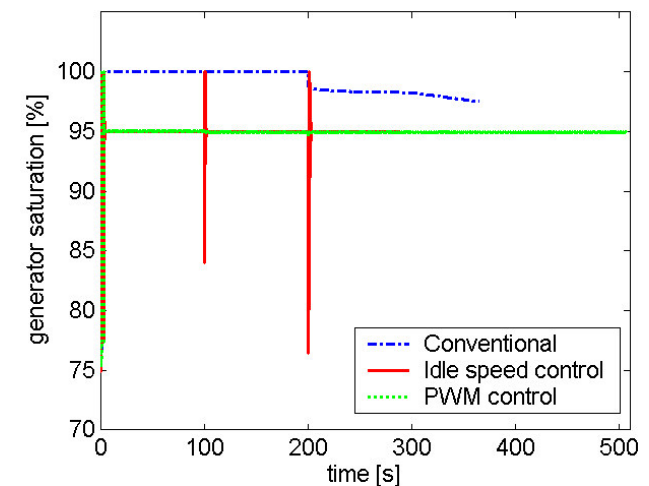
(SOC) is taken 70% and the initial temperature equal to that of the frozen windscreen: -3°C .

For the simulations the initial condition is a vehicle that has a frozen windscreen (-3°C , $200\mu\text{m}$ thick ice layer). The electrical heated windscreen will be activated after 3 seconds after the simulation is initiated. The simulation will be stopped when the outer surface temperature of the heated windscreen has reached 3°C . The complete simulation will take place with the engine in idle state. The output data of interest is (i) the cumulative fuel consumption, (ii) the voltage of the power net, (iii) the engine idle speed and (iv) the time before the outer surface temperature of the windscreen has reached 3°C . The results for the three different strategies are as follows:

7.1 Voltage Stability and Generator Saturation



(a)



(b)

Fig. 18 (a) Powernet voltage for the three different strategies, (b) generator saturation

It can be seen from Fig. 18a that operating the electric heated windscreen with the conventional strategy

will result in losing control of the powernet voltage. It can be seen in Fig. 18b that this is caused by the fact that the generator is saturated in this case. The amount of power requested by the electric powernet exceeds in the conventional case the power that can be delivered by the generator. Therefore the generator setpoint can not be followed and the powernet voltage will drop to the battery voltage. After 200 seconds the glow plugs will become inactive and the generator is from this point on able to supply the total requested electric power and therefore follow its voltage setpoint.

With the two other strategies (*i.e.* idle speed control and PWM control), the generator saturation can be controlled to 95% and therefore the voltage of the powernet can be maintained at 14.2V.

7.2 Effect of Engine Idle Speed Control

Since the second strategy makes use of engine idle speed control to increase the generator output, it is interesting to see the difference in the engine speed for the three strategies. Fig. 19 shows this. Where the engine speed remains 750 rpm with the conventional and the PWM controlled strategy, the engine speed with the idle speed control strategy is increased to improve the generator output. The stepped decrease of the engine speed can be explained by the residual loads (cf. Section 5.4): 55A from 0-100s, 40A during 100-200s and 20A after 200s.

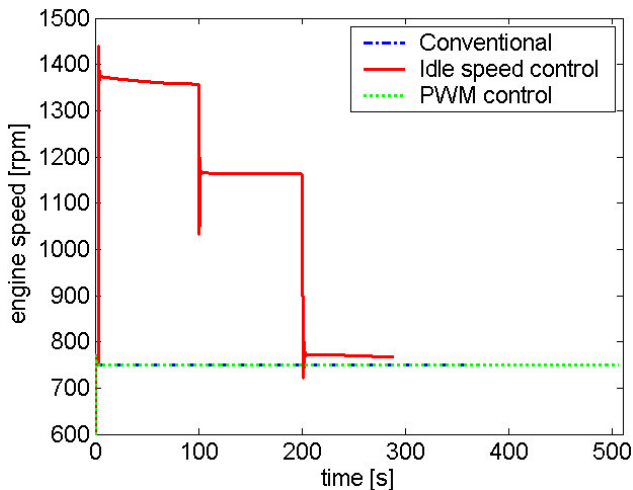


Fig. 19 The effect of engine idle speed control

7.3 Effect of PWM Control

As discussed in Section 6.3, adding a PWM switch to the heated windscreen can be used to reduce the load and therefore maintain powernet voltage stability. Dependent on the amount of power requested,

the generator saturation is controlled to 95% by changing the PWM frequency of the electric heated windscreen. Fig. 20 shows the simulated PWM frequency. Again the steps are caused by the reduction of the residual loads (as also explained in the previous section).

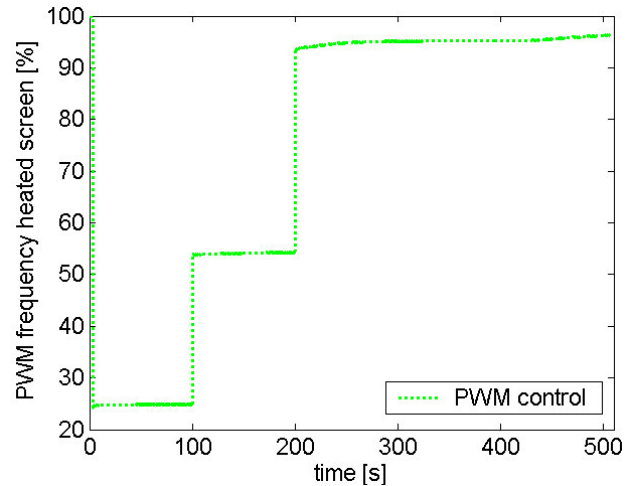


Fig. 20 Percentage of maximum load that the electric heated windscreen is operated with (PWM)

7.4 Heating Performance and Fuel Economy

Other factors of interest are the time before the temperature of the outer surface of the heated screen has reached 3°C and how many fuel is used until this point is reached. Fig. 21 shows the temperature of the outer surface: the phase transition from ice to water can be clearly seen. There is a significant difference between the three strategies: the strategy with idle speed control is the fastest (total time is 290 seconds), followed by the conventional strategy (total time is 365 seconds) and the PWM controlled strategy (total time is 507 seconds).

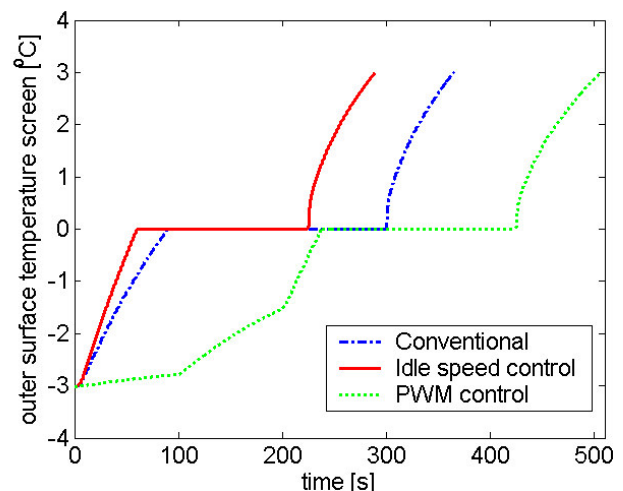


Fig. 21 Outer surface temperature of the electric heated windscreen.

The cumulative fuel consumption during the heating of the frontscreen is displayed in Fig. 22. The gradient for the idle speed control can be explained by the fact that the fuel consumption at higher engine speeds is larger (due to engine / transmission / generator losses). The total amount of fuel used is: 50 gram for the conventional strategy, 52 gram for idle speed control and 69 gram for the PWM controlled case.

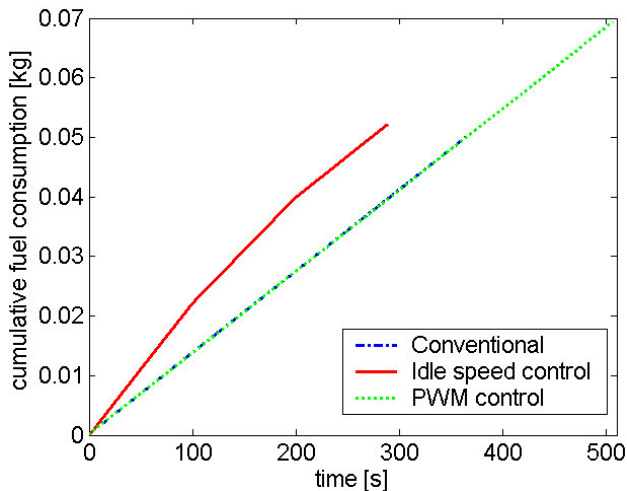


Fig. 22 Cumulative fuel consumption during the heating process

7.5 Summarized Results

The following table summarizes the results from the previous subsections.

Table 1 Summarized results

	Conv.	Idle speed	PWM
Stable voltage? (yes/no)	NO	YES	YES
Time to reach 3°C [s]	365	290	590
Fuel used [g]	50	52	69

By controlling the idle speed, the voltage can be kept stable, the (time) performance of the heated windscreen can be increased and that all without paying a fuel penalty compared with the conventional strategy. An important issue with idle speed control however is customer perception: *e.g.* noise quality issues. Since different eigenfrequency modes of vehicle systems (*e.g.* body, powertrain) will reside in the engine speed range, it should be prevented to control to idle speeds that induce such eigenfrequencies. Dependent on vehicle application and engine type, it therefore is necessary to investigate the idle speed range that is usable for idle speed control. A thought can be to omit different idle speed ranges by defining not-

allowed engine speed bands, and as such prevent getting a vehicle system in an eigenfrequency.

Acknowledgements

The authors wish to thank Eckhard Karden, battery expert of the Energy Management Group of Ford Forschungszentrum Aachen and Dirk Uwe Sauer of the RWTH Aachen University for their great ideas in battery modeling. Also Daniel Kok, Michael Tiller, Serve Ploumen, Maurice Rienks and Thomas Gerhards are thanked for their support and ideas.

References

1. **Tiller, M., Bowles, P. and Dempsey, M.**, "Development of a Vehicle Model Architecture in Modelica", ", Proceedings of the 3rd International Modelica Conference, pp. 75-85, Linköping Sweden, 2003
http://www.modelica.org/Conference2003/papers/h32_vehicle_Tiller.pdf
2. **Surewaard, E., Tiller, M. and Linzen, D.**, "A Comparison of Different Methods for Battery and Supercapacitor Modeling", SAE paper 2003-01-2290, 2003
3. **Surewaard, E., Karden, E. and Tiller, M.**, "Advanced Electric Storage System Modeling in Modelica", Proceedings of the 3rd International Modelica Conference, pp. 95-102, Linköping Sweden, 2003
http://www.modelica.org/Conference2003/papers/h11_Surewaard.pdf
4. **Surewaard, E., Kok, D., and Tiller, M.**, "Engine Cranking: Advanced Modeling and an Investigation of the Influence of the Initial Crank Angle and Inertia", SAE paper 2004-01-1875, 2004
5. **Thele, M., Buller, S., Sauer, D.U., De Doncker, R.W. and Karden, E.**, "Hybrid Modeling of Lead-Acid Batteries in Frequency and Time Domain", Journal of Power Sources, In press, 2005
6. **Bode, H.**, "Lead-acid Batteries", Wiley, 1977
7. **Graf, A.**, "Power Semiconductors to Drive Energy Management", Second Aachener Elektroniksymposium, Institut fuer Kraftfahrwesen, Aachen, 2004
8. **Rienks, M. and Kok, D.**, "Development and Implementation of Electrical Power Distribution Management", Second Aachener Elektroniksymposium, Institut fuer Kraftfahrwesen, Aachen, 2004